ELSEVIER

Journal of Fluids and Structures 25 (2009) 1282–1298

JOURNAL OF FLUIDS AND STRUCTURES

www.elsevier.com/locate/jfs

A vorticity formulation for computational fluid dynamic and aeroelastic analyses of viscous flows

L. Morino*, G. Bernardini, G. Caputi-Gennaro

Università Roma Tre, Dipartimento di Ingegneria Meccanica e Industriale, Via della Vasca Navale 79, I-00146 Rome, Italy

Received 17 February 2008; accepted 21 July 2009
Available online 12 September 2009

Abstract

The paper deals with a novel computational formulation for the analysis of viscous flows past a solid body. The formulation is based upon a convenient decomposition of the flow field into potential and rotational velocity contributions, which has the distinguishing feature that the rotational velocity vanishes in much of, if not all, the region in which the vorticity is negligible. Contrary to related formulations implemented by the authors in the past, in the proposed approach, discontinuities of the potential and rotational velocity fields across a prescribed surface emanating from the trailing edge (such as the wake mid-surface) are eliminated, thereby facilitating numerical implementations. However, the main novelty is related to the application of the boundary condition: first, the expression for the velocity used for the condition on the body boundary is consistent with that for the velocity in the field; also—contrary to related formulations used by the authors in the past—in the proposed approach, the condition on the body boundary does not require the evaluation of the total vorticity (inside and outside the computational domain). The proposed algorithm, valid for three-dimensional compressible flows, is validated—as a first step—for the case of two-dimensional incompressible flows. Specifically, numerical results are presented for the aerodynamic analysis of two-dimensional incompressible viscous flows past a circular cylinder and past a Joukowski airfoil. In order to verify the desirable absence of artificial damping, we present also results pertaining to the flutter (i.e., dynamic aeroelastic) analysis of a spring-mounted circular cylinder in a viscous flow, free to move in a direction orthogonal to the unperturbed flow. In both cases (aerodynamics and aeroelasticity), the results are in good agreement with existing literature data.

Keywords: Computational fluid dynamics; Viscous flow; Aeroelasticity; Irrotational/vortical-field decomposition

1. Introduction

This paper presents a novel computational methodology for the analysis of viscous flows, based upon an exact decomposition of the velocity field into an irrotational and a rotational contribution. The methodology is particularly advantageous for exterior flows (e.g., flows around wings). Hence, this is the only case addressed here, although the concepts are applicable to interior flows as well. The numerical results presented here are limited to the case of two-dimensional incompressible viscous flows. Thus, only the corresponding formulation is presented in detail.

*Corresponding author. Fax: +39 06 5593732.
E-mail addresses: L.Morino@uniroma3.it (L. Morino), g.bernardini@uniroma3.it (G. Bernardini), giovanni.CAPUTI@bridgestone.eu (G. Caputi-Gennaro).

0889-9746/$ - see front matter © 2009 Elsevier Ltd. All rights reserved.
doi:10.1016/j.jfluidstructs.2009.07.004

However, for the sake of completeness, the theoretical formulation, valid for unsteady three-dimensional compressible viscous flows, is outlined in Appendix A, primarily as a motivation for introducing the methodology and to present the full potentiality and the ultimate objective of the work.

The main driver of this work is the consideration that—as well known—the analysis of high-Reynolds-number attached flows around streamlined bodies is considerably simplified if the flow field may be assumed to be primarily irrotational. Indeed, it is well known that—at least for incompressible and subsonic flows—the potential-flow problem may be solved quite efficiently by boundary-element methods, in particular, by the approach introduced by Morino (1974) and reviewed in Morino and Tseng (1990), Morino and Gennaretti (1992), and Morino (2003). In order to retain such an efficiency, the case of attached high-Reynolds-number flows is typically studied simply by modifying the potential-flow analysis by including a viscous-flow correction. This is usually accomplished by using either one of the two well known methods, introduced by Lighthill (1958) for three-dimensional incompressible flows: (i) the displacement-thickness method, or (ii) the equivalent-source method (now commonly known as the transpiration-velocity method, see Lemmerman and Sonnad (1979), who extended the technique to three-dimensional steady compressible flows). However, the Lighthill approaches (very useful to evaluate the correction to potential-flow results due to the presence of the boundary layer and indeed widely used in practical applications) are limited by the standard boundary-layer assumption (that is, small thickness of the rotational region).

In order to overcome this limitation (for instance, to study the Navier–Stokes equations for separated flows), one may use formulations in non-primitive variables (that is, vorticity based), which are not limited by the boundary-layer approximation. In this approach, the flow field is divided into two regions: (i) the *irrotational* region (defined here as the region where the vorticity is negligible), and (ii) its complement, the *vortical* region. The primary advantage of the non-primitive-variable approach over the computational solution of the Navier–Stokes equations in primitive variables (i.e., velocity and pressure) is the fact that, for exterior flows, the computational domain for the former (that is, the *vortical* region) is typically much smaller when compared to that for the latter (that is, the entire fluid volume). Indeed, this is the primary reason why we believe that vorticity-based formulations are particularly interesting for exterior flows.

Any formulation in non-primitive variables is based upon a general class of potential/vorticity decompositions of the type

$$\mathbf{v} = \nabla\varphi + \mathbf{w}, \tag{1}$$

where $\mathbf{w}$ is any particular solution of the equation

$$\nabla \times \mathbf{w} = \boldsymbol{\zeta}, \tag{2}$$

with $\boldsymbol{\zeta} \coloneqq \nabla \times \mathbf{v}$ denoting the vorticity field.[1] Eq. (1) states that the flow field may be decomposed into two contributions, one related to the vorticity (called the *vortical* velocity), the other being irrotational (called the *potential* velocity).

The class of potential/vorticity decompositions is very broad and includes, in particular, the Helmholtz decomposition, for which the vortical velocity contribution, $\mathbf{w}$, is the curl of a vector field, $\boldsymbol{\psi}$, the so-called vector potential [see, e.g., Serrin (1959)]. As pointed out by Morino (1990), the problem with such a decomposition—in applications to unsteady viscous compressible flows—is that both the scalar potential and the vector potential are governed by the Poisson equation, and not by the wave equation as one might expect for unsteady compressible flows: thus, the physical phenomenon of sound propagation is completely hidden by the mathematical representation provided by the Helmholtz decomposition. Specifically, the vector-potential contribution is solenoidal and, therefore, has an infinite speed of propagation. The implication is that the vector-potential contribution does not vanish in the irrotational region. Hence, in such a region, the scalar-potential contribution includes a term equal and opposite to the vector-potential contribution, all through the term $\Theta \coloneqq \nabla \cdot \mathbf{v}$. As a consequence, the source terms in the equation for the scalar-potential (see Eq. (A.2)) are different from zero in a rather large region, thereby causing a deterioration in the efficiency of the method. In physical terms, in the Helmholtz decomposition the vortical-velocity representation implies that a change in the vorticity distribution causes an instantaneous change of the vortical velocity throughout the flow field. Thus, the potential velocity has to perform a double work: first, subtract the contribution of the vortical contribution and then add the finite-speed propagation of the disturbance—all of this, by using the Poisson equation and not the wave equation!

In order to avoid this problem, it is desirable to have a decomposition in which the rotational velocity, $\mathbf{w}$—and hence the source term, $\Theta = -\nabla \cdot \mathbf{w}$, see Eq. (14)—vanishes in much of the irrotational region. Indeed, the potential velocity may be obtained by boundary-element methods, which retain their efficiency even in the presence of source terms in the flow field, provided that these terms are limited to a relatively small field region. This fact is the key to the relevance of

[1] Eq. (2) must necessarily be satisfied, as it is seen by taking the curl of Eq. (1). On the other hand, Eq. (2) is also a sufficient condition: for, it is apparent that $\mathbf{v} - \mathbf{w}$ is irrotational, and hence potential, thereby proving the validity of Eq. (1).

the proposed formulation. As a key by-product, we have that for compressible flows the potential velocity represents explicitly the propagation mechanism of the vorticity-generated sound (see Appendix A).

2. Problems in past related work

A decomposition having $\mathbf{w} = \mathbf{0}$ in much of, if not all, the irrotational region is used here. In order to put the paper in the proper perspective, the past work of the authors and their collaborators is critically reviewed here (and examined in detail in Section 3), so as to provide the motivation for the present work, by identifying the preceding limitations that are being overcome here. The distinguishing feature of the various approaches used in all these works (including the present one) is the fact that $\mathbf{w}$ is obtained by direct integration of Eq. (2), as explicitly indicated in Eq. (A.4). This in turn requires using a suitable direction of integration (as discussed below); the difference between different approaches introduced in the past consists of the direction of integration utilized.

In the following, as stated above, we limit ourselves to two-dimensional flows (the three-dimensional ones being addressed in Appendix A). Thus, in order to discuss the different approaches, we have to specify the coordinate system used. In the case of two-dimensional steady viscous flows around an object, the vortical region (boundary layer and wake) has a limited extent (a few chord lengths in the case of an airfoil). On the contrary, in the case of unsteady viscous flows, the vorticity extends considerably beyond the object. Hence, for the computational analysis of unsteady flows, it is convenient to use a curvilinear coordinate system elongated in the direction of the flow, that is, a *C*-grid. Specifically, consider a line $\mathscr{L}_W$ which starts from the trailing edge and extends to infinity. It is convenient that $\mathscr{L}_W$ be directed—more or less—like the flow; thus, $\mathscr{L}_W$ is close to the middle of the wake and it will be referred to as the *wake mid-line* (even though, strictly speaking, this may be only approximately true). Next, we introduce a body-fitted system of curvilinear coordinates ξ and η, with

$$\mathbf{x} = \mathbf{x}(\xi, \eta), \tag{3}$$

such that the line $\eta = 0$ coincides with the union of the body contour $\mathscr{C}_B$ with the two sides of the wake mid-line $\mathscr{L}_W$ (whereas $\|\mathbf{x}\| \to \infty$, as $\eta \to \infty$).

Related formulations presented in the past may be divided into two groups. In the first group [introduced by Morino and Beauchamp (1988) and Beauchamp (1990) for two-dimensional incompressible flows, and extended to three-dimensional compressible flows in Morino (1990)], the integration is in the ξ-direction (that is, approximately in the direction of the flow). Here, it will be referred to as *Scheme A*. In the second group [introduced by Morino et al. (1999) and implemented by Arsuffi et al. (2001) and Morino et al. (2003) for two-dimensional incompressible flows], the integration is in the η-direction (that is, along the normal to the body boundary and to the wake mid-line). Here, it will be referred to as *Scheme B*. As shown in Morino et al. (1999), the formulation resulting from this second approach is closely related to the classical coupling of potential and boundary-layer flows, through the Lighthill (1958) transpiration-velocity approach.

As pointed out in detail in Section 3.2, both Scheme A and Scheme B yield, across the wake mid-line, equal and opposite discontinuities in the two contributions (potential and vortical) of the velocity, thereby rendering the numerical application of both formulations quite cumbersome to use. Specifically, in Scheme A, $\mathbf{w}$ is discontinuous unless the $J\boldsymbol{\zeta}$ field is symmetric (where J is the Jacobian of the transformation $\mathbf{x} = \mathbf{x}(\xi, \eta)$), whereas, in Scheme B, $\mathbf{w}$ is discontinuous unless the $J\boldsymbol{\zeta}$ field is antisymmetric (that is, unless the flow field is symmetric). A third approach that eliminates these problems was proposed in Morino and Bernardini (2002) (see Scheme C in Section 3.2). This will referred to as *Scheme C* and consists of dividing the field $J\boldsymbol{\zeta}$ into two contributions that are, respectively, symmetric and antisymmetric with respect to the coordinate η. Then, for the symmetric portion of $J\boldsymbol{\zeta}$, $\mathbf{w}$ is obtained using Scheme A, that is, by integrating along the ξ-direction, whereas for the antisymmetric portion, $\mathbf{w}$ is obtained using Scheme B, that is, by integrating along the η-direction. The resulting vortical velocity field $\mathbf{w}$ is continuous, thereby eliminating discontinuities also in the potential velocity, $\nabla\varphi$. This paper presents the first numerical results for the validation of Scheme C, with applications to aerodynamics and aeroelasticity (Section 4).

However, as mentioned above, the main novelty in the present paper is in the approach used to impose the body boundary condition. In order to cast this issue in the proper perspective, recall that in all the non-primitive variable formulations, the boundary condition is imposed by expressing the velocity at the boundary (or inside the boundary) in terms of the vorticity distribution (in the field and on the boundary); then, imposing the no-slip condition one obtains the values of the vorticity at the boundary. The various approaches available differ by the velocity–vorticity relationship used [see, for instance, Wu (1976), Morino (1985, 1990), Quartapelle (1993), Guj and Stella (1993), Cossu (1997), and Cossu and Morino (1997)].

It may be noted that in the last two formulations, a single velocity–vorticity relationship, that based upon the Biot–Savart law [which arises from the Helmholtz decomposition, see Morino (1985)], is used for the evaluation of both the velocity in the field and that at the boundary (i.e., for imposing the no-slip condition). In other words, the evaluation of the velocity in the field and the no-slip boundary condition are mutually consistent. A consistent approach is also used in the above-mentioned implementations of Scheme A (Morino and Beauchamp, 1988; Beauchamp, 1990). On the contrary, in the implementations of Scheme B (Arsuffi et al., 2001; Morino et al., 2003), there is an inconsistency between the approach used to evaluate the velocity in the field and that for the no-slip boundary condition. Specifically, Scheme B (that is, Eq. (1), with **w** given by Eq. (13)) is used only for evaluating the velocity in the field, whereas the Biot–Savart implementation of Cossu (1997) is utilized for the no-slip condition.

In Arsuffi et al. (2001) and Morino et al. (2003), such an approach is indicated, as "very preliminary" and to be replaced by an approach in which the algorithm utilized for the boundary condition is consistent with that used to evaluate the velocity in the field. Such an approach is employed here: the direct integration algorithm is used for both, the evaluation of the velocity in the field and the implementation of the no-slip boundary condition.

It should be emphasized that, as pointed out by Wu (1976) and addressed in details by Cossu and Morino (1997), for two-dimensional flows the system of equations that yields the nodal values of the boundary vorticity is singular and hence an additional condition must be imposed: the conservation of the total vorticity which stems from the Stokes and Kelvin theorems (since the vorticity vanishes exponentially at infinity)

$$\frac{\mathrm{d}}{\mathrm{d}t}\iint_{\mathbb{R}^2}\zeta\,\mathrm{d}\mathscr{A}=\frac{\mathrm{d}}{\mathrm{d}t}\iint_{\mathscr{A}_F}\zeta\,\mathrm{d}\mathscr{A}+2\frac{\mathrm{d}\Omega}{\mathrm{d}t}\mathscr{A}_S=0, \tag{4}$$

where we have used $\mathbb{R}^2=\mathscr{A}_F\cup\mathscr{A}_S$, with $\mathscr{A}_F$ and $\mathscr{A}_S$ denoting, respectively, the fluid and the solid regions (the latter is assumed for simplicity to be rigid), whereas $\Omega=\frac{1}{2}\zeta$ is the angular velocity of the body.

Finally, in past implementations, the computational domain is limited to a region relatively close to the solid body. Hence, imposing the total-vorticity conservation requires the evaluation of the amount of vorticity that leaves the computational domain. This implies that inaccuracies in the evaluation of the vorticity that leaves the computational domain affect the amount of vorticity generated at the boundary. For this reason, the total-vorticity-conservation condition is here replaced by an equivalent one that does not require the evaluation of the vorticity leaving the computational domain. This is the most interesting novel theoretical contribution of the present paper and is addressed in Section 3.4.

3. Theoretical formulation and numerical implementation

As mentioned above, the ultimate goal of the present work is the analysis of three-dimensional unsteady compressible viscous flows and the present paper should be seen just as a very first (although crucial) step towards that direction. Specifically, the numerical applications presented here are limited to two-dimensional incompressible flows. For this reason the formulation presented in the main body of the paper is limited to two-dimensional incompressible flows (the extension to three-dimensional compressible flows is briefly addressed in Appendix A, simply to convey to the reader the full potentiality of the proposed approach).

Consider a two-dimensional incompressible flow past a solid body having arbitrary shape and arbitrary motion. The governing equations are the continuity equation

$$\nabla\cdot\mathbf{v}=0\quad(\mathbf{x}\in\mathscr{A}_F) \tag{5}$$

and the Navier–Stokes equations. These, using the dimensionless variables $\mathbf{v}=\check{\mathbf{v}}/U_\infty$, $p=\check{p}/\rho U_\infty^2$, $\mathbf{x}=\check{\mathbf{x}}/\ell$ and $t=U_\infty\check{t}/\ell$ (where U_∞ is the undisturbed velocity, ℓ is a suitable reference length, and ρ is the density, whereas $\check{}$ denotes physical variables), are given by

$$\frac{D\mathbf{v}}{Dt}\coloneqq\frac{\partial\mathbf{v}}{\partial t}+(\mathbf{v}\cdot\nabla)\mathbf{v}=-\nabla p+\frac{1}{\mathrm{Re}}\nabla^2\mathbf{v}\quad(\mathbf{x}\in\mathscr{A}_F), \tag{6}$$

with Re denoting the Reynolds number: $\mathrm{Re}=U_\infty\ell/\nu$, where ν is the kinematic viscosity coefficient.

To complete the problem, we need the boundary conditions on the contour of the body, $\mathscr{C}_B$,

$$\mathbf{v}=\mathbf{v}_B\quad(\mathbf{x}\in\mathscr{C}_B), \tag{7}$$

and those at infinity, which in a frame of reference rigidly connected with the undisturbed fluid (undisturbed-fluid frame of reference) are given by (Kress, 1989)

$$\mathbf{v} = o(\|\mathbf{x}\|^{-1}) \quad \text{and} \quad p - p_\infty = o(1) \ \ (\text{as } \|\mathbf{x}\| \longrightarrow \infty) \tag{8}$$

(where, for any a and b, $a = o(b)$ means that a/b tends to zero). In addition, we have the initial condition; assuming to start from rest, this is[2]

$$\mathbf{v}(\mathbf{x}, 0) = \mathbf{0}. \tag{9}$$

The solution of these equations through the use of Eq. (1) requires the solution of four separate problems: (i) the evaluation of the vorticity ζ in the field, (ii) the evaluation of the vortical velocity $\mathbf{w}$ from ζ, (iii) the evaluation of the potential φ, (iv) the evaluation of ζ at the boundary.

3.1. Evaluation of the vorticity in the field

The first problem requires simply the solution of the two-dimensional vorticity transport equation. This is obtained as the curl of the Navier–Stokes equations, Eq. (6), and, for two-dimensional flows, is given by

$$\frac{D\zeta}{Dt} \coloneqq \frac{\partial \zeta}{\partial t} + \mathbf{v} \cdot \nabla \zeta = \frac{1}{\mathrm{Re}} \nabla^2 \zeta. \tag{10}$$

This equation is spatially discretized by central finite differences (with the Laplacian represented by its standard tensor-analysis expression for curvilinear non-orthogonal coordinates). For the time integration, the (inefficient, but convenient) explicit Euler scheme is used.

3.2. Evaluation of $\mathbf{w}$

Eq. (10) requires the availability of the values of the velocity only at the field nodes, where the discretized form of Eq. (10) is being used to evaluate the vorticity. As a consequence, the evaluation of the velocity is to be performed only in the vortical region.

In this subsection, we consider the formulation for the vortical contribution $\mathbf{w}$ (φ is considered in the next subsection). In a two-dimensional flow, Eq. (2) yields only one non-zero component, that is,

$$J\zeta = \frac{\partial w_2}{\partial \xi} - \frac{\partial w_1}{\partial \eta}, \tag{11}$$

where ζ is the (two-dimensional) vorticity, whereas w_1 and w_2 are the covariant components of $\mathbf{w}$. This equation may be solved by assuming—arbitrarily but legitimately (Morino, 1990)—one of the two covariant components of $\mathbf{w}$ to vanish, and by integrating Eq. (11) in a suitable direction (the same holds true for three-dimensional flows, see Eq. (A.4)). The three schemes outlined in Section 2 are illustrated in detail in the following.

Scheme A: The first scheme (Morino and Beauchamp, 1988; Beauchamp, 1990; Morino, 1990) consists of choosing $w_1(\xi, \eta) = 0$. Hence, integrating Eq. (11) yields

$$w_1(\xi, \eta) = 0, \quad w_2(\xi, \eta) = -\int_{\xi}^{\infty} J(\check{\xi}, \eta)\zeta(\check{\xi}, \eta)\, \mathrm{d}\check{\xi}. \tag{12}$$

The most important consequence of this last equation—key to the formulation—is that the vortical velocity contribution $\mathbf{w}$ vanishes in much of the irrotational region. Specifically, given an arbitrary point $\mathbf{x}$, we have that $\mathbf{w}(\mathbf{x}) = \mathbf{0}$, if $\zeta = 0$ for all the points on the η-line between $\mathbf{x}$ and infinity (that is, in much of, if not all, the irrotational region, given the above choice of the coordinates ξ and η). It is easy to verify that this approach yields a normal discontinuity for $\mathbf{w}$ across the mid-wake line $\mathscr{L}_W$, unless $J\zeta$ is symmetric with respect to η [see Morino and Bernardini (2002)]. Therefore, the formulation is cumbersome to use in practical applications.

[2] In general, one may assume that $\mathbf{v}(\mathbf{x}, 0) = \mathbf{v}_0(\mathbf{x})$, provided that the total vorticity (including that of the solid region) is initially zero, so as to have that the potential φ is single-valued at all times (this may be seen from the Kelvin theorem applied to a contour that surrounds the vortical region).

Scheme B: The second scheme (Morino et al., 1999, 2003) consists of choosing $w_2(\xi,\eta)=0$. Hence, integrating Eq. (11) yields

$$w_1(\xi,\eta)=\int_\eta^\infty J(\xi,\check{\eta})\zeta(\xi,\check{\eta})\,\mathrm{d}\check{\eta},\quad w_2(\xi,\eta)=0. \tag{13}$$

Again, we have $\mathbf{w}=0$ in much of (if not all) the irrotational region. It is also easy to verify that the use of this scheme yields a tangential discontinuity for $\mathbf{w}$ across the mid-wake line $\mathscr{L}_W$, unless $J\zeta$ is antisymmetric with respect to the η-direction [as in the case of symmetric flows; see again Morino and Bernardini (2002)]. Therefore, the formulation is cumbersome to use in practical applications, except for the case of symmetric flows.

Scheme C: As mentioned above, the remedy used here consists of decomposing the field $J\zeta$ into two contributions, one symmetric and the other one antisymmetric with respect to the variable η, and to use Scheme A for the symmetric contribution and Scheme B for the antisymmetric one. This procedure eliminates any $\mathbf{w}$ discontinuity across the mid-wake line $\mathscr{L}_W$ [it may be noted that the same considerations apply for the three-dimensional case; see again Morino and Bernardini (2002)].

In all three schemes, the integral in Eq. (12) and/or (13) is performed by using the Simpson rule.

3.3. Evaluation of φ

Next, consider the formulation for the potential contribution introduced by Eq. (1). Combining the incompressible-flow continuity equation, Eq. (5), with the expression for the velocity, Eq. (1), yields

$$\nabla^2\varphi=\Theta\quad(\mathbf{x}\in\mathscr{A}_F), \tag{14}$$

where $\Theta:=-\nabla\cdot\mathbf{w}$.

Next, consider the boundary condition for φ on the boundary contour $\mathscr{C}_B$. Dotting Eq. (7) with the outer normal to $\mathscr{C}_B$, $\mathbf{n}$, one obtains $\mathbf{v}\cdot\mathbf{n}=\mathbf{v}_B\cdot\mathbf{n}$ for $\mathbf{x}\in\mathscr{C}_B$. Then, using Eq. (1), we have

$$\frac{\partial\varphi}{\partial n}=\chi-\mathbf{w}\cdot\mathbf{n}\quad(\mathbf{x}\in\mathscr{C}_B), \tag{15}$$

where $\chi:=\mathbf{v}_B\cdot\mathbf{n}$. In addition, in a frame of reference connected with the undisturbed fluid, we have $\varphi=o(1)$ at infinity.[3]

Recalling that, in Scheme C proposed here, $\mathbf{w}$ is continuous by construction, we have that $\nabla\varphi$ is also continuous everywhere in the field, and so is φ, since, as mentioned in footnote 2, here φ is single-valued. Thus, the boundary integral representation for the Poisson equation, Eq. (14), with the above boundary condition at infinity, is given by

$$\varphi(\mathbf{x})=\oint_{\mathscr{C}_B}\left(\frac{\partial\varphi}{\partial n}G-\varphi\frac{\partial G}{\partial n}\right)\mathrm{d}s(\mathbf{y})+\iint_{\mathscr{A}_\mathbf{w}}G\Theta\,\mathrm{d}\mathscr{A}(\mathbf{y}), \tag{16}$$

with $\mathscr{A}_\mathbf{w}$ denoting the region where $\mathbf{w}\neq\mathbf{0}$, whereas $G=\ln\|\mathbf{x}-\mathbf{y}\|/2\pi$ and $\partial/\partial n=\nabla_\mathbf{y}\cdot\mathbf{n}(\mathbf{y})$ ($\nabla_\mathbf{y}$ denotes that we are taking the gradient with respect to $\mathbf{y}$). Eq. (16) allows one to evaluate φ everywhere in the field, if φ and $\partial\varphi/\partial n$ over $\mathscr{C}_B$ and Θ in $\mathscr{A}_\mathbf{w}$ are known.

However, only $\partial\varphi/\partial n$ is prescribed by the boundary conditions, Eq. (15). Therefore, we need an equation to evaluate φ on $\mathscr{C}_B$. With this in mind, note that, in the limit, as $\mathbf{x}$ tends to $\mathscr{C}_B$, Eq. (16) yields a compatibility condition between φ and $\partial\varphi/\partial n$ on $\mathscr{C}_B$ and Θ in $\mathscr{A}_\mathbf{w}$. In our case, this compatibility condition corresponds to an integral equation, which allows one to evaluate φ on $\mathscr{C}_B$, provided that $\partial\varphi/\partial n$ on $\mathscr{C}_B$ and Θ in $\mathscr{A}_\mathbf{w}$ are known (Morino, 2003).

Note that, following Beauchamp (1990), one may perform an integration by parts on the field integral, and obtain

$$\varphi(\mathbf{x})=\oint_{\mathscr{C}_B}\left(\chi G-\varphi\frac{\partial G}{\partial n}\right)\mathrm{d}s(\mathbf{y})+\iint_{\mathscr{A}_\mathbf{w}}\nabla G\cdot\mathbf{w}\,\mathrm{d}\mathscr{A}(\mathbf{y}), \tag{17}$$

which shows that the contribution from $\mathbf{w}$ (and hence ζ) may be expressed in terms of a doublet distribution in $\mathscr{A}_\mathbf{w}$, in the direction of $\mathbf{w}$ and intensity $\|\mathbf{w}\|$. In the limit as the wake thickness tends to zero, this yields the standard formulation for quasi-potential flows with a doublet-layer wake (Morino, 1990).

[3]For the Laplace equation, this requires $\oint_{\mathscr{C}_B}(\partial\varphi/\partial n)\,\mathrm{d}s=0$ (Kress, 1989) (see Eq. (16), where $G=\ln r/2\pi$ tends to infinity as $\|\mathbf{x}\|\to\infty$). For rigid bodies, we have $\oint_{\mathscr{C}_B}\chi\,\mathrm{d}s=0$. The question is then—do we have to impose $\oint_{\mathscr{C}_B}\mathbf{w}\cdot\mathbf{n}\,\mathrm{d}s=0$ as well? The answer is: no. The reason is that here, instead of the Laplace equation, we have the Poisson equation, Eq. (14), with $\Theta:=-\nabla\cdot\mathbf{w}$. This yields a compensation between the line source integral and the field integral, with the result that, as $\|\mathbf{x}\|\to\infty$, φ tends indeed to zero, as apparent from Eq. (17).

In the numerical applications, in order to avoid singularities, Eq. (17) is discretized by using a piecewise cubic scheme (Hermite interpolation) on $\mathscr{C}_B$, whereas in the field a piecewise linear scheme is used.

3.4. Evaluation of the vorticity at the boundary

Finally, consider the evaluation of the vorticity at the body-boundary nodes. The procedure presented here is the main theoretical novelty introduced in this paper.

As for any vorticity-based method, a problem arises for the vorticity boundary condition. This condition is not directly available, whereas available is the condition on the velocity, Eq. (7). Therefore, in order to obtain the desired condition for the vorticity at the boundary, it is necessary to express the velocity boundary condition in Eq. (7) in terms of ζ. As mentioned above, in Arsuffi et al. (2001) and Morino et al. (2003), this problem has been approached by using the implementation of Cossu (1997) of the Biot–Savart law. However, this approach confers a hybrid aspect to the formulation—that is, the direct-integration approach is used to evaluate $\mathbf{w}$ in the field and the Biot–Savart law on the boundary.

On the contrary, the formulation used here to impose the boundary condition is the same as that utilized to evaluate the velocity in the field (Section 3.2). Given the future objective (compressible flows), this is a key validation point because the Biot–Savart law is valid only for incompressible flows.

In order to discuss this formulation, note that—were the vorticity completely known—the velocity would be known except for the potential contribution, Eq. (1), and hence only one boundary condition would have to be imposed [see, for instance, Batchelor (1967, pp. 87 and 104)]. Hence, we may impose Eq. (15).[4]

However, in our case, the vorticity is not completely known, since the vorticity at the boundary is still to be determined. Hence, a deeper analysis is needed. For the sake of clarity, consider first symmetric flows. Then, given $\partial\varphi/\partial n$ from Eq. (15) and Θ in the field, the integral equation for φ, obtained from Eq. (16) as $\mathbf{x}$ tends to $\mathscr{C}_B$, yields a velocity distribution that does not necessarily satisfy the no-slip condition

$$(\nabla\varphi + \mathbf{w} - \mathbf{v}_B)\cdot\mathbf{t} = 0, \tag{18}$$

where $\mathbf{t}$ denotes the tangential unit vector on $\mathscr{C}_B$. The reason for this is that an arbitrary vorticity distribution does not necessarily correspond to a velocity field that satisfies the no-slip condition.

The standard interpretation of the term $(\nabla\varphi + \mathbf{w} - \mathbf{v}_B)\cdot\mathbf{t}$ is that of a velocity discontinuity between the fluid and the solid region. However, in our case, it is convenient to adopt the following point of view: there exists a zero-thickness vortex layer of intensity

$$\gamma = (\nabla\varphi + \mathbf{w} - \mathbf{v}_B)\cdot\mathbf{t}, \tag{19}$$

and this vortex layer—although adjacent to $\mathscr{C}_B$—is fully contained in the flow field (Morino, 1986, 1990).

In the approach used in Morino and Beauchamp (1988), Beauchamp (1990) and Morino (1990) this layer immediately diffuses, thereby yielding that the no-slip condition is automatically satisfied (for, if it was not, there would be a zero-thickness vortex layer).[5] This approach is adopted here.

Next, consider non-symmetric flows. The algorithm proposed for symmetric flows is not applicable to non-symmetric (lifting) flows, because, in this case, the total vorticity generated over the boundary ought to be, in general, different from zero, whereas, with the above approach, we have that

$$\oint_{\mathscr{C}_B}\gamma\,\mathrm{d}s = \oint_{\mathscr{C}_B}\nabla\varphi\cdot\mathrm{d}\mathbf{x} + \oint_{\mathscr{C}_B}\mathbf{w}\cdot\mathrm{d}\mathbf{x} - \oint_{\mathscr{C}_B}\mathbf{v}_B\cdot\mathrm{d}\mathbf{x} = 0. \tag{20}$$

Indeed, the first term vanishes, since

$$\oint_{\mathscr{C}_B}\nabla\varphi\cdot\mathrm{d}\mathbf{x} = \oint_{\mathscr{C}_B}\mathrm{d}\varphi = 0, \tag{21}$$

[4]The formulation discussed here is for two-dimensional problems. However, similar results hold for three-dimensional flows as well. It should be noted that, for the three-dimensional case, there exists an issue which is rarely addressed in the literature: the unknown vorticity on the boundary consists of a thin vortex layer that is solenoidal and therefore depends upon a single scalar distribution over the boundary surface. Hence, it is sufficient (and appropriate) to use the normal boundary condition to obtain the solution [for a deeper analysis of this subtle point, the reader is referred to Morino (1990)].

[5]In other words, here vorticity generation and diffusion are treated as independent process (as in "operator splitting"). On the contrary, in formulations based on the Helmholtz decomposition [such as Wu (1976), Cossu (1997), and Cossu and Morino (1997, 1999)] one deals with a layer of distributed vorticity (that is, the process of vorticity generation and diffusion are considered to be simultaneous).

because, as mentioned above, in the present formulation φ is single-valued. In addition, the contour integral of $\mathbf{w}$ vanishes; for, $d\mathbf{x} = \mathbf{g}_1\, d\xi$ and hence $\mathbf{w}\cdot d\mathbf{x} = w_1\, d\xi$, where $w_1 = 0$ for the symmetric portion of $J\zeta$, whereas, for the antisymmetric one, it is the contour integral that vanishes. Finally, the last term vanishes, because $\mathbf{v}_B$ is independent from $\mathbf{x}$, whereas $\oint_{\mathscr{C}_B} d\mathbf{x} = \mathbf{0}$.

The remedy is provided by the fact that the total vorticity must remain constant, as indicated explicitly in Eq. (4). Specifically, as mentioned above, in viscous flows the vortex layer generated on the body contour is convected and diffused in the fluid field. This requires that we introduce suitable changes in the vorticity at the boundary, so that the total vorticity remains constant, in agreement with Eq. (4).

In Cossu (1997), this condition is imposed through an evaluation of the "outgoing vorticity" (that is, the vorticity that leaves the computational domain through the outer boundary). This approach makes the scheme highly sensitive: indeed, small errors in the evaluation of the outgoing vorticity may pile up, over time, and alter the vorticity generated—at every time step—at the inner boundary; this in turn requires that the evaluation of the outgoing vorticity must be very accurate—not an easy task, since the outer boundary is where we have the lowest computational accuracy, because of the coarseness of the computational grid there.

The novel approach proposed here for overcoming this drawback is based upon the evaluation of the vorticity flux from the body to the field through a contour $\mathscr{C}_*$ that is close to the inner boundary. Such a flux must be compensated for by an opposite variation of the vorticity on the boundary.

In order to clarify this issue and obtain an explicit expression for the vorticity to be added on $\mathscr{C}_B$ [and show the equivalence to the formulation of Cossu (1997)], let us divide the fluid region into two parts, one inside and the other outside the contour $\mathscr{C}_*$, denoted, respectively, by $\mathscr{A}_F^I$ and $\mathscr{A}_F^E$, so that $\mathscr{A}_F = \mathscr{A}_F^I \cup \mathscr{A}_F^E$. Using the Leibniz theorem for an integral with moving boundaries, as well as the vorticity transport equation, Eq. (10), and the continuity equation, $\nabla\cdot\mathbf{v} = 0$, one obtains

$$\begin{aligned}\frac{d}{dt}\iint_{\mathscr{A}_F^E}\zeta\, d\mathscr{A} &= \iint_{\mathscr{A}_F^E}\frac{\partial\zeta}{\partial t}\, d\mathscr{A} - \oint_{\mathscr{C}_*}\zeta\mathbf{v}_*\cdot\mathbf{n}\, ds = \iint_{\mathscr{A}_F^E}\frac{D\zeta}{Dt}\, d\mathscr{A} - \oint_{\mathscr{C}_*}\zeta(\mathbf{v}_*-\mathbf{v})\cdot\mathbf{n}\, ds\\ &= -\oint_{\mathscr{C}_*}\left(\nu\frac{\partial\zeta}{\partial n} + \zeta(\mathbf{v}_*-\mathbf{v})\cdot\mathbf{n}\right) ds,\end{aligned} \tag{22}$$

where $\mathbf{v}_*$ is the velocity of a point of the contour $\mathscr{C}_*$, whereas $\mathbf{n}$ points from $\mathscr{A}_F^I$ to $\mathscr{A}_F^E$. Eq. (22) allows one to evaluate the total vorticity variation in the fluid region external to $\mathscr{C}_*$. Recalling now Eq. (4) and that $\mathscr{A}_F = \mathscr{A}_F^I \cup \mathscr{A}_F^E$, we have finally

$$\frac{d}{dt}\iint_{\mathscr{A}_F^I}\zeta\, d\mathscr{A} = \oint_{\mathscr{C}_*}\left(\nu\frac{\partial\zeta}{\partial n} + (\mathbf{v}_*-\mathbf{v})\cdot\mathbf{n}\zeta\right) ds - 2\frac{d\Omega}{dt}\mathscr{A}_S. \tag{23}$$

Eq. (23) represents the time-variation of the total vorticity inside $\mathscr{C}_*$. Of course, as apparent from the derivation above, this is completely equivalent to imposing the total vorticity conservation, Eq. (4), since this was used in the derivation of Eq. (23). In the computational implementation, we choose for $\mathscr{C}_*$ to be defined by the equation $\eta = \frac{1}{2}\eta_1$, where η_1 is the value of η corresponding to the first set of field nodes away from the body boundary (in other words, $\mathscr{C}_*$ is located between the boundary and the first set of nodes). Then, Eq. (23) yields the total vorticity to be added in the region $\mathscr{A}_F^I$. This vorticity may be distributed arbitrarily among the various boundary nodes, because the arbitrariness is subsequently compensated for by the vorticity distribution obtained from Eq. (19).

A second-order scheme is used for the spatial discretization of Eq. (23).

4. Validation

In view of the novelty of the scheme, it is necessary to validate and assess the accuracy and the efficiency of the algorithm. To this aim, we considered first steady incompressible two-dimensional flows and compared the results against data either available in the literature, or obtained using commercial codes (Section 4.1). Second, we considered unsteady incompressible flows, specifically, the transient response of the flow around a circular cylinder subject to an impulsive start (Section 4.2).

Next note that, in the case of unsteady phenomena, two aspects should be kept in mind: (i) it is possible that the numerical scheme introduces instabilities that are not present in the original operator—this is typically referred to as the "numerical-instability" problem; and (ii) it is also possible that the numerical scheme introduces damping—this is typically referred to as the "artificial-damping" problem. The unsteady aerodynamic analysis validates the first issue (the numerical-instability problem), but not the second one (the artificial-damping problem). This second issue is particularly important in fluid–solid interaction, because a physical instability might be camouflaged by the artificial

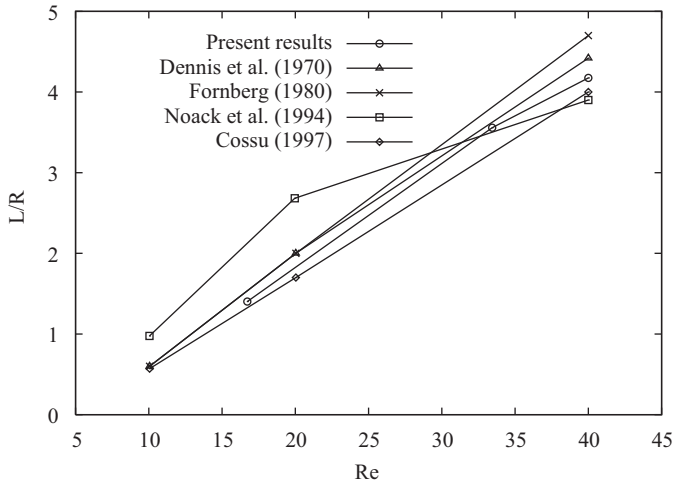

Fig. 1. Steady state: recirculation bubble length versus Reynolds number.

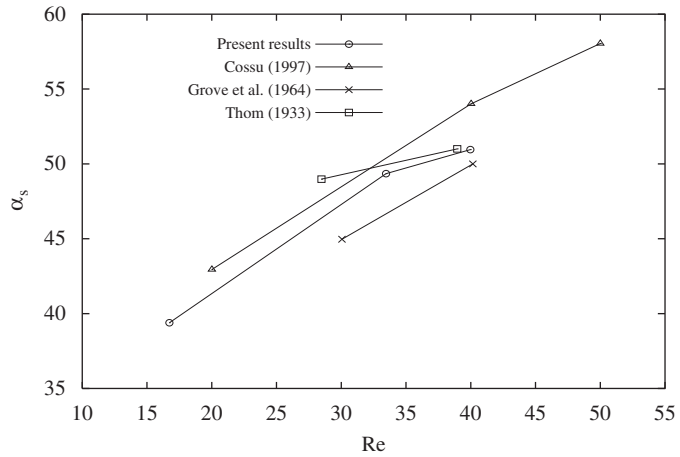

Fig. 2. Steady state: separation angle versus Reynolds number.

damping introduced by the numerical scheme. Thus, third, the validation includes an aeroelastic analysis in the neighborhood of the flutter boundary (Section 4.3). A conformal-mapping C-grid (Ives, 1982) is used for all the results.

4.1. Steady aerodynamics

In order to validate the formulation for steady incompressible flows, we considered, as test cases, a circular cylinder, as well as an airfoil in a uniform flow.

The first test case considered is a circular cylinder (having diameter D) in a uniform flow, for which extensive results are available. In Figs. 1–3, the numerical results obtained are compared to those available in the literature. Specifically, Fig. 1 depicts the dimensionless length of the recirculation bubble (that is, the distance of the singular point from the cylinder, along the x-axis), as a function of $\mathrm{Re} := U_\infty D/\nu$. The present results are in good agreement with the numerical results of Dennis and Chang (1970), Fornberg (1980) and Cossu (1997) and to a lesser extent with those of Noack and Eckelmann (1994). Fig. 2 depicts the separation-point angle as a function of the Reynolds number. Our results are compared with the experimental ones by Thom (1933) and Grove et al. (1964), and the numerical ones by Cossu (1997), which are obtained by using the Biot–Savart law. Again, the agreement is satisfactory.[6] Fig. 3 depicts the vorticity

[6]It may be added that the numerical results by Fornberg (1980) and Dennis and Chang (1970), not shown in the figure for the sake of clarity, are quite close to those by Cossu (1997).

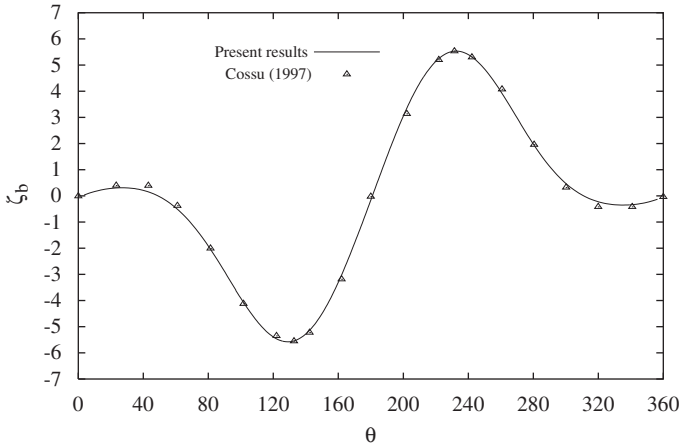

Fig. 3. Steady state: wall vorticity.

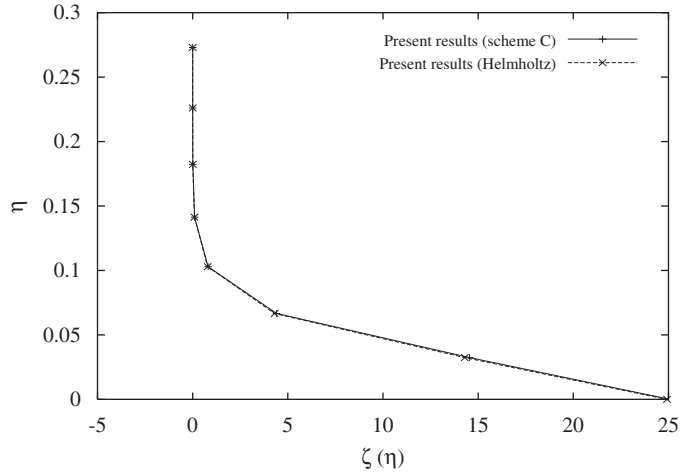

Fig. 4. Airfoil in steady state: vorticity at $\xi = 0.25$ (quarter chord) for $\mathrm{Re} = 40$ and $\alpha = 3^\circ$.

distribution along the cylinder boundary for $\mathrm{Re} = 16.712$ ($\theta = 0^\circ$ corresponds to the downstream point). Note that the symmetry of the flow is correctly captured. The results are compared to the only ones found in the literature [i.e., Cossu (1997) and Cossu and Morino (1997)]. The agreement is quite good; the present results are obtained by using a C-grid with 100 elements in the ξ-direction (20 elements on either side of the body, 30 along the wake) and 20 elements in theη-direction; on the other hand, those of Cossu (1997) are obtained by using an O-grid with 80 elements in the ξ-direction and 40 in the (radial) η-direction.

The second test case considered is a symmetric Joukowski airfoil in a uniform flow. An airfoil at zero angle of attack does not provide a good test for Scheme C (because in this case the flow is symmetric, and hence Scheme C reduces to Scheme B). Thus, the test case used is that of an airfoil (having chord c) at an angle of attack $\alpha = 3^\circ$, with $\mathrm{Re}:=U_\infty c/\nu = 40$. A C-grid is used, with—on each side—60 elements in the ξ-direction (30 elements on each side of the airfoil) and 30 in the η-direction. Figs. 4 and 5 show a comparison between the present results and those obtained by the authors, by using the Biot–Savart law formulation that was presented in Cossu and Morino (1997). Specifically, Fig. 4 depicts $\zeta = \zeta(0.25, \eta)$, as a function of η (quarter-chord vorticity profile). Furthermore, Fig. 5 depicts the velocity covariant component, $v_1(0.25, \eta)$, as a function of η (quarter-chord profile of v_1). In addition, Figs. 6 and 7 show a comparison between the present results and those obtained by the authors, by using the commercial code Fluent 5.5 (1999) (the results obtained by the authors with the Biot–Savart law formulation are not shown, since they are identical—within plotting accuracy—to the present ones). Specifically, Fig. 6 depicts the pressure coefficient along the airfoil boundary, Eq. (A.1) whereas Fig. 7 presents the vorticity distribution also along the airfoil boundary. In both

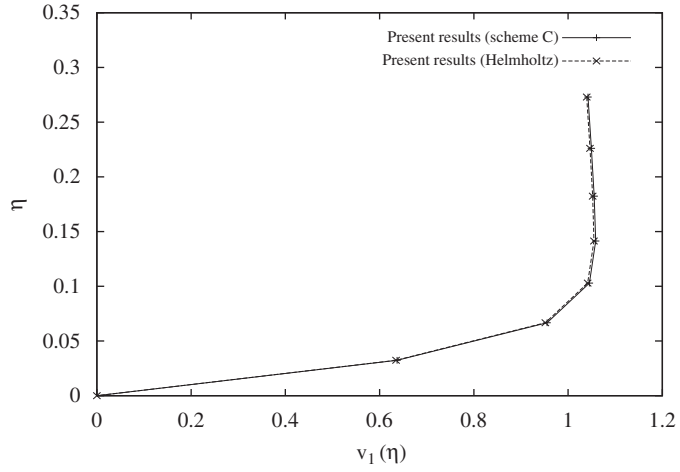

Fig. 5. Airfoil in steady state: velocity at $\xi = 0.25$ (quarter chord) for $\mathrm{Re} = 40$ and $\alpha = 3^\circ$.

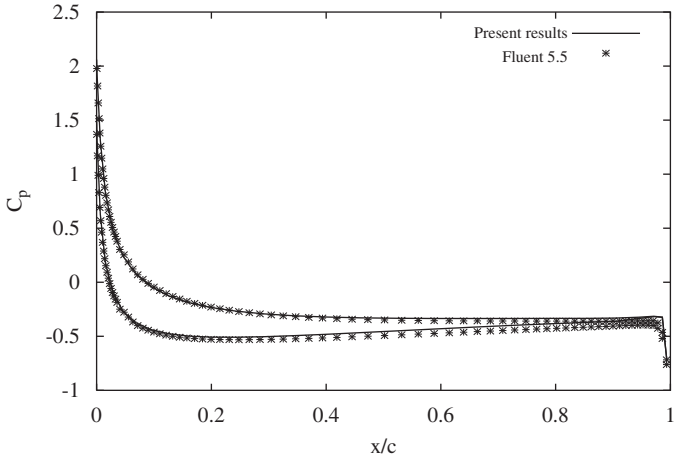

Fig. 6. Airfoil in steady state: wall pressure coefficient for $\mathrm{Re} = 40$ and $\alpha = 3^\circ$.

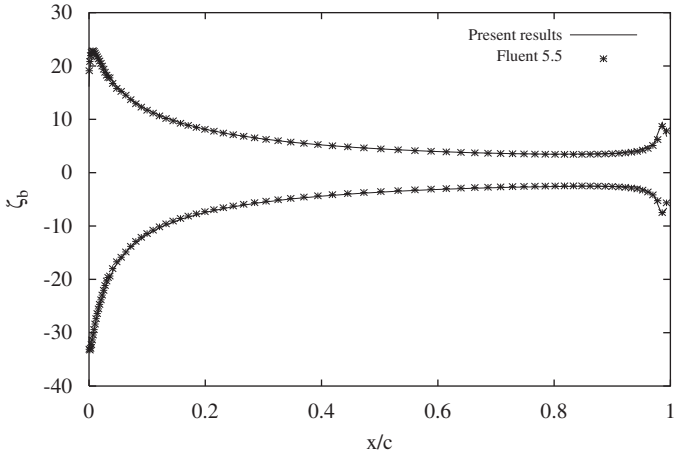

Fig. 7. Airfoil in steady state: wall vorticity for $\mathrm{Re} = 40$ and $\alpha = 3^\circ$.

Table 1
Comparison of results obtained by the present work with those obtained numerically with Fluent 5.5.

	C_l	C_d	C_{mo}
Present work	0.1477	0.72266	−0.0413
Fluent 5.5	0.1635	0.72070	−0.0453

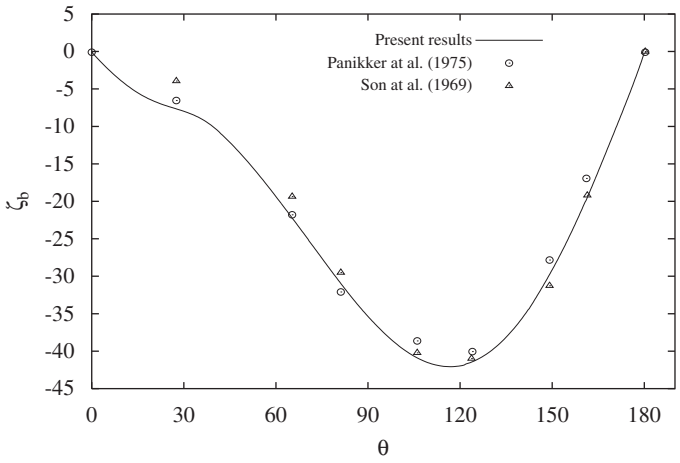

Fig. 8. Impulsive start: wall vorticity at $t = 0.15$, for $\mathrm{Re} = 500$.

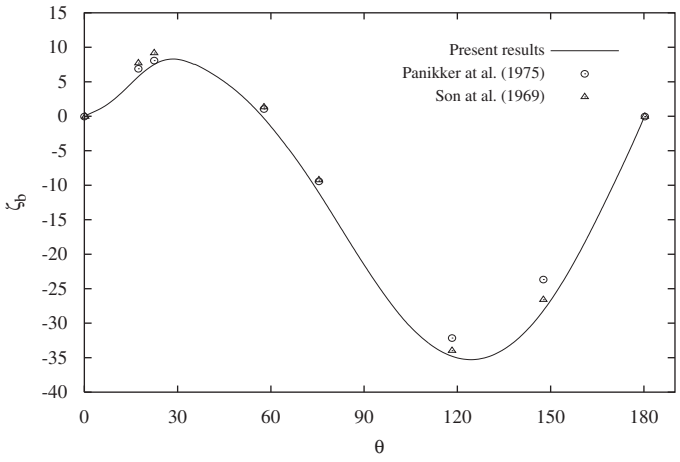

Fig. 9. Impulsive start: wall vorticity at $t = 0.5$, for $\mathrm{Re} = 500$.

cases, the agreement is remarkably good, especially those regarding the vorticity distribution. In addition, Table 1 shows the comparison in terms of aerodynamic coefficients between the present results and those obtained by the authors, again by using Fluent 5.5 (1999). The forces are obtained by integrating both the shear stress and the pressure distributions along the body contour

$$\mathbf{f} = \oint_{\mathscr{C}_B} (-p\mathbf{n} + \tau\mathbf{t})\,\mathrm{d}s, \tag{24}$$

where $\tau = \mu\zeta$, whereas p is obtained by using again Eq. (A.1). The agreement is quite satisfactory, although—strangely enough—not as much as the non-integrated data. Further analysis of this issue is deemed desirable.

4.2. Unsteady aerodynamics

In order to validate the formulation for unsteady aerodynamics, we considered the problem of an impulsive start of a circular cylinder, for Re = 500. The results obtained are presented in Figs. 8 and 9, which depict—for dimensionless time $t = U_\infty \check{t}/D = 0.15$ and $t = 0.50$, respectively—the distribution of the vorticity ζ along the contour of the cylinder (that is, as a function of the angle θ, with $\theta = 0^\circ$ identifying the downstream point of the cylinder). Note that, because of the symmetry of the flow, the vorticity is an antisymmetric function of θ. The results obtained by Son and Hanratty (1969) and by Panikker and Lavan (1975) are also shown in Figs. 8 and 9. The comparison is quite satisfactory—the differences between the three methods are of the same order of magnitude.

4.3. Flutter

As mentioned above, in order to make sure that the numerical scheme (which is stable, as implicitly validated in the preceding subsection) does not introduce artificial damping, it is convenient to consider a validation based upon a fluid–solid interaction that includes an estimate of the instability boundary. Thus, an aeroelastic (flutter) analysis has been performed. The physical model examined consists of a rigid spring-dashpot-mounted cylinder, in a uniform incompressible flow having undisturbed velocity $U_\infty \mathbf{i}$. The only degree of freedom of the cylinder is in the direction orthogonal to the undisturbed flow. The mathematical model is presented in Section 4.3.1, the numerical results in Section 4.3.2.

4.3.1. Aeroelastic model

The equation governing the motion of a rigid cylinder having a single elastic degree of freedom, subject to a spring-dashpot force and the fluid pressure, is given by [see, for instance, Belvins (1991)]

$$\frac{\mathrm{d}^2 y}{\mathrm{d}t^2} + \gamma \frac{\mathrm{d}y}{\mathrm{d}t} + \omega_C^2 y = \frac{\kappa}{\pi} c_L, \tag{25}$$

where $t = U_\infty \check{t}/D$ is the dimensionless time and $y = \check{y}/D$ is the dimensionless displacement of the cylinder, whereas ω_C is the dimensionless structural natural frequency, γ the dimensionless damping coefficient of the cylinder, $\kappa = \rho_F/\rho_C$ the fluid/solid density ratio, and $c_L = L/\frac{1}{2}\rho_F U_\infty^2 D$ the cylinder lift coefficient per unit length. The lift is evaluated using Eq. (24).

The Newmark (1959)-β method is used for the numerical integration of Eq. (25).

4.3.2. Numerical results

The simulations assume that, for negative times, the cylinder is at rest, surrounded by a steady-state viscous flow (numerically, this steady state is obtained through a transient with the cylinder held fixed). At time $t = 0$, a sudden impulse is applied to the cylinder, so that, at $t = 0^+$, we have $y = 0$, but $v = \mathrm{d}y/\mathrm{d}t = 0.035$ [as in Cossu and Morino

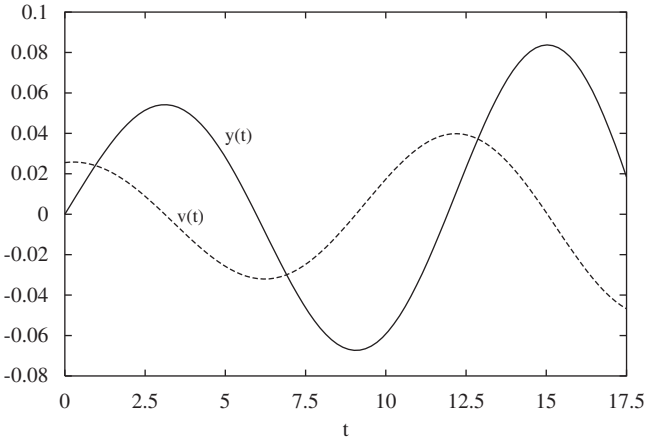

Fig. 10. Displacement and velocity versus t, for Re = 23.512, $\kappa = \frac{1}{7}$, $\gamma = 0.01$, $\omega_C = 4.88$.

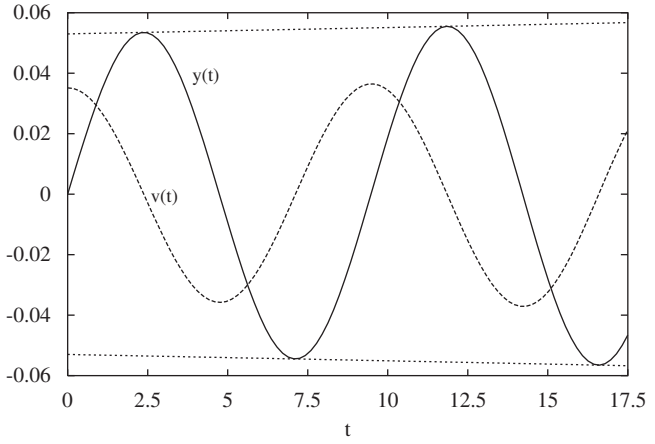

Fig. 11. Displacement and velocity versus t, for $\mathrm{Re} = 23.512$, $\kappa = \frac{1}{70}$, $\gamma = 0.01$, $\omega_C = 4.88$.

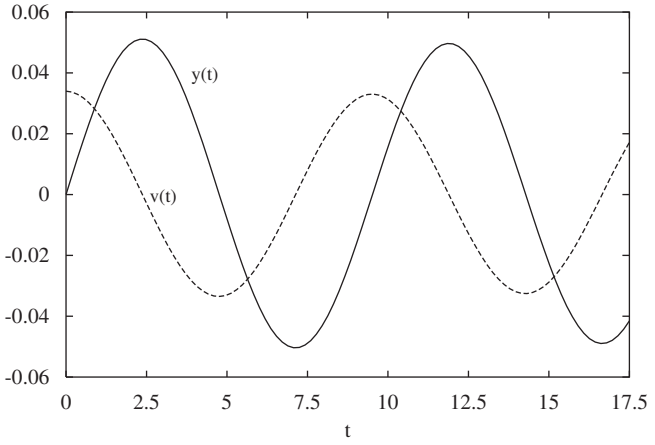

Fig. 12. Displacement and velocity versus t, for $\mathrm{Re} = 23.512$, $\kappa = \frac{1}{7000}$, $\gamma = 0.01$, $\omega_C = 4.88$.

(1999)]. For comparison, the same values used by Cossu and Morino (1999) were assumed for Re, ω_C, and γ (that is, $\mathrm{Re} = 23.512$, $\omega_C = 4.88$, and $\gamma = 0.01$). The transient responses are shown in Figs. 10–12, respectively, for $\kappa = \frac{1}{7}, \frac{1}{70}, \frac{1}{7000}$.

The first case is definitely unstable, the third is definitely stable, the second is near the stability boundary. For this last case, further analysis was performed. Specifically, for the case $\kappa = \frac{1}{70}$, we estimated the logarithmic decrement and the oscillation period of the response, thereby obtaining the real and imaginary parts of the critical pole, respectively, $\alpha = 3.7 \times 10^{-2}$ and $\omega = 0.663$ (of course this presumes that the unsteady part of the solution is close to that of a linear operator; this is true here because the amplitude of oscillation is small). Both of these values are in excellent agreement with the values reported in Cossu and Morino (1999), $\alpha = 3.803 \times 10^{-2}$ and $\omega = 0.660$ (obtained via an eigenvalue analysis of the equations linearized around the steady-state solution).

5. Concluding remarks

A convenient decomposition for the analysis of viscous flows has been presented. This falls within the vast class of potential/vorticity decomposition of the type $\mathbf{v} = \nabla\varphi + \mathbf{w}$, which includes the classical Helmholtz decomposition as a particular case. A distinguishing feature of the present decomposition is that the vortical velocity contribution $\mathbf{w}$ (obtained by a line integration along a suitable path) vanishes in much of the irrotational region. As a consequence, in

much of the irrotational region one obtains $\mathbf{v} = \nabla\varphi$. The paper presents three novelties with respect to preceding work by the authors and their collaborators.

The first novelty is an implementation and assessment of the formulation by Morino and Bernardini (2002), where the rotational velocity is obtained by separating the field $J\zeta$ into two contributions that are symmetric and antisymmetric with respect to the coordinate η, normal to the body and the mid-wake line (then, in evaluating $\mathbf{w}$, the most convenient direction of integration is chosen for each of the two contributions, as discussed in Section 3.2). The advantage of this approach is that the rotational velocity field (and hence the potential one) is continuous across the wake, thereby facilitating the numerical implementation. The computational results obtained indicate that the accuracy of the formulation is superior to that of earlier approaches (Schemes A and B) and that the implementation does not present any of the cumbersome aspects of either scheme.

The second novelty introduced here is in the formulation of the boundary conditions, where we use the same velocity–vorticity formulation for both evaluating the field velocity and imposing the boundary conditions (in preceding works, a hybrid, very preliminary, approach was used, with the Biot–Savart law employed for imposing the boundary conditions). Again, the assessment is very satisfactory in terms of accuracy and the resulting formulation is self-consistent—as already pointed out, this is an essential item of the validation, given the ultimate objective of the work, since the use of the Biot–Savart law for compressible flows is cumbersome.

As a third novelty, the condition of constant total vorticity is replaced by an equivalent one that does not require the evaluation of the vorticity that leaves the computational domain (see Section 3.4). This novelty as well yields a considerable streamlining of the scheme, since the wake region may be reduced considerably without loss of accuracy, because the total vorticity in the field is no longer evaluated in the new scheme.

In addition, numerical results have been presented. These include analyses of: (i) steady aerodynamics, (ii) unsteady aerodynamics, and (iii) flutter. These analyses allowed us to verify also the absence of both numerical instabilities and artificial damping. The results are in good agreement with existing data, thereby providing a satisfactory, albeit preliminary, validation of the formulation.

Further work deemed necessary includes convergence analyses and, ultimately, the implementation and validation of the formulation for three-dimensional compressible flows, which is outlined in Appendix A.

Appendix A. Three-dimensional compressible formulation

In this appendix the formulation for the case of compressible viscous flows is addressed; for details, see Morino (2003). Assuming the body forces and the heat sources to be negligible, the governing equations are (Serrin, 1959) the continuity equation $\mathrm{D}\rho/Dt + \rho\nabla\cdot\mathbf{v} = 0$, the Navier–Stokes equations, $\rho D\mathbf{v}/Dt = -\nabla p + \mathrm{div}\,\mathbf{V}$ (where $\mathbf{V}$ is the viscous-stress tensor), and the entropy transport equation, $\rho T DS/Dt = \mathbf{V}:\mathbf{D} - \nabla\cdot\mathbf{q}$ (where T is the temperature of the fluid, $\mathbf{D}$ the strain rate tensor, and $\mathbf{q}$ the heat flux vector). In addition, recall that $\mathrm{d}h = T\mathrm{d}S + \mathrm{d}p/\rho$, where h denotes the enthalpy, and hence, $\nabla p/\rho = \nabla h - T\nabla S$. Next, combining the last equation with the Navier–Stokes equations, and recalling the expression for the acceleration, $D\mathbf{v}/Dt = \partial\mathbf{v}/\partial t + \frac{1}{2}\nabla v^2 + \boldsymbol{\zeta}\times\mathbf{v}$, yields a generalized Bernoulli theorem introduced by Morino (1985):

$$\dot{\varphi} + \frac{v^2}{2} + h + \lambda = h_\infty, \tag{A.1}$$

where $\lambda(\mathbf{x}) = \int_\infty^{\mathbf{x}} \mathbf{r}(\mathbf{y})\cdot\mathrm{d}\mathbf{y}$, with $\mathbf{r} = \partial\mathbf{w}/\partial t + \boldsymbol{\zeta}\times\mathbf{v} - T\nabla S - \mathrm{Div}\,\mathbf{V}/\rho$, where the integral is path independent.

Next, consider the equation for the potential φ. Combining the continuity equation with Eqs. (1) and (A.1), and the equation of state $\rho = \rho(h, S)$, one obtains

$$\nabla^2\varphi - \frac{1}{a_\infty^2}\frac{\partial^2\varphi}{\partial t^2} = \sigma, \tag{A.2}$$

where σ includes all the terms due to the presence of the vorticity and viscosity, as well as the nonlinear terms in the potential-flow formulation (Morino, 2003).

The solution of Eq. (A.2) may be obtained using a standard boundary element method [see, in particular, Morino (2003)]. In this case, it is apparent that: (i) it is desirable to have $\mathbf{w} = 0$, as much as possible, in the irrotational region, so as to reduce the volume of integration, and (ii) avoid discontinuities for $\mathbf{w}$, so as to have $\nabla\varphi$ and φ continuous as well, thereby eliminating the surface integral over the mid-wake surface.

This may be accomplished as follows. Introduce suitable curvilinear coordinates, ξ^α, and the transformation $\mathbf{x} = \mathbf{x}(\xi^\alpha, t)$, invertible everywhere. Eq. (2), in curvilinear coordinates, reads

$$J\zeta^1 = \frac{\partial w_3}{\partial \xi^2} - \frac{\partial w_2}{\partial \xi^3}, \quad J\zeta^2 = \frac{\partial w_1}{\partial \xi^3} - \frac{\partial w_3}{\partial \xi^1}, \quad J\zeta^3 = \frac{\partial w_2}{\partial \xi^1} - \frac{\partial w_1}{\partial \xi^2}, \tag{A.3}$$

where J is the Jacobian of the transformation $\mathbf{x} = \mathbf{x}(\xi^\alpha, t)$. Next, choose, arbitrarily $w_1 = 0$.[7] Then, integrating Eq. (A.3) along a ξ^1-line, one obtains

$$w_1(\xi^1, \xi^2, \xi^3) = 0,$$

$$w_2(\xi^1, \xi^2, \xi^3) = -\int_{\xi^1}^{\infty} J\zeta^3(\hat{\xi}^1, \xi^2, \xi^3)\, \mathrm{d}\hat{\xi}^1,$$

$$w_3(\xi^1, \xi^2, \xi^3) = \int_{\xi^1}^{\infty} J\zeta^2(\hat{\xi}^1, \xi^2, \xi^3)\, \mathrm{d}\hat{\xi}^1. \tag{A.4}$$

The considerations presented in the main body of the paper—regarding the direction of integration (Scheme C) and the numerical implementation—apply to this case as well.

References

Arsuffi, G., Baragona, M., Bernardini, G., Morino, L., 2001. A computational formulation for the analysis of viscous flows with aeroelastic applications. In: XVI Congresso Nazionale AIDAA (Associazione Italiana Di Aeronautica e Astronautica). Palermo, Italy.

Batchelor, G.K., 1967. An Introduction to Fluid Dynamics. Cambridge University Press, Cambridge.

Beauchamp, P.P., 1990. A potential-vorticity decomposition for the boundary integral equation analysis of viscous flows. Ph.D. Thesis, Graduate School, Boston University.

Belvins, R.D., 1991. Flow-induced Vibrations. Van Nostrand Reinhold, New York.

Cossu, C., 1997. Analisi di stabilitá lineare e non-lineare del flusso viscoso intorno ad un cilindro circolare. Ph.D. Dissertation, Dipartimento di Ingegneria Aerospaziale, Università degli Studi di Roma La Sapienza, Roma, Italy.

Cossu, C., Morino, L., 1997. A vorticity-only formulation and a low-order asymptotic expansion solution near Hopf bifurcation. Computational Mechanics 20, 229–241.

Cossu, C., Morino, L., 1999. On the instability of a spring-mounted circular cylinder in a viscous flow at low Reynolds numbers. Journal of Fluids and Structures 13, 1–15.

Dennis, S.C.R., Chang, G.Z., 1970. Numerical solutions for steady flow past a circular cylinder at Reynolds numbers up to 100. Journal of Fluid Mechanics 42, 471–489.

Fluent 5.5, 1999. User's guide. Fluent Inc., Lebanon, NH.

Fornberg, B., 1980. A numerical study of steady viscous flow past a circular cylinder. Journal of Fluid Mechanics 98, 819–855.

Grove, A.S., Shair, F.H., Petersen, E.E., Acrivos, A., 1964. An experimental investigation of the steady separated flow past a circular cylinder. Journal of Fluid Mechanics 19, 60–80.

Guj, G., Stella, F., 1993. A vorticity-velocity method for the numerical solution of 3D incompressible flows. Journal of Computational Physics 106 (2), 286–298.

Ives, D.C., 1982. Conformal grid generation. In: Thompson, J.F. (Ed.), Numerical Grid Generation. North-Holland, Amsterdam.

Kress, R., 1989. Linear Integral Equations. Springer, Berlin.

Lemmerman, L.A., Sonnad, V.R., 1979. Three-dimensional viscous-inviscid coupling using surface transpiration. Journal of Aircraft 16 (6), 353–358.

Lighthill, M.J., 1958. On displacement thickness. Journal of Fluid Mechanics 4, 383–392.

Morino, L., 1974. A general theory of compressible potential aerodynamics. NASA CR-2464.

Morino, L., 1985. Scalar/vector potential formulation for compressible viscous unsteady flows. NASA CR-3921.

Morino, L., 1986. Helmholtz decomposition revisited: vorticity generation and trailing edge condition. Computational Mechanics 1, 65–90.

[7]This is legitimate because the first equation in Eq. (A.3) is automatically satisfied by Eq. (A.4). Indeed, using $J\nabla\cdot\boldsymbol{\zeta} = \partial(J\zeta^\alpha)/\partial\xi^\alpha = 0$, we have

$$\frac{\partial w_3}{\partial \xi^2} - \frac{\partial w_2}{\partial \xi^3} = \int_{\mathbf{x}}^{\infty} \left(\frac{\partial}{\partial \xi^2}(J\zeta^2) + \frac{\partial}{\partial \xi^3}(J\zeta^3) \right) \mathrm{d}\xi^1 = -\int_{\mathbf{x}}^{\infty} \frac{\partial}{\partial \xi^1}(J\zeta^1)\, \mathrm{d}\xi^1 = J\zeta^1.$$

Morino, L., 1990. Helmholtz and Poincaré potential-vorticity decompositions for the analysis of unsteady compressible viscous flows. In: Banerjee, P.K., Morino, L. (Eds.), Developments in Boundary Element Methods, Nonlinear Problems of Fluid Dynamics, vol. 6. Elsevier Applied Science Publishers, Barking, UK.

Morino, L., 2003. Is there a difference between aeroacoustics and aerodynamics? An aeroelastician's viewpoint. AIAA Journal 41 (7), 1209–1223.

Morino, L., Beauchamp, P.P., 1988. A potential-vorticity decomposition for the analysis of viscous flows. In: Tanaka, M., Cruse, T.A. (Eds.), Boundary Element Methods in Applied Mechanics (Proceeding of First Joint Japan/US Symposium on Boundary Element Methods). Pergamon Press, Tokyo.

Morino, L., Tseng, K., 1990. A general integral formulation for unsteady compressible potential flows with applications to airplane and rotors. In: Banerjee, P.K., Morino, L. (Eds.), Developments in Boundary Element Methods, Nonlinear Problems of Fluid Dynamics, vol. 6. Elsevier Applied Science Publishers, Barking, UK, pp. 183–246.

Morino, L., Gennaretti, M., 1992. Boundary integral equation methods for aerodynamics. In S.N. Atluri (Ed.), Computational Nonlinear Mechanics in Aerospace Engineering, AIAA Progress in Aeronautics and Astronautics, 146, pp. 279–321.

Morino, L., Bernardini, G., 2002. On the vorticity generated sound for moving surfaces. Computational Mechanics 28 (3–4), 311–316.

Morino, L., Salvatore, F., Gennaretti, M., 1999. A new velocity decomposition for viscous flows: Lighthill equivalent-source method revisited. Computer Methods in Applied Mechanics and Engineering 173 (3–4), 317–336.

Morino, L., Bernardini, G., Baragona, M., 2003. A viscous-flow decomposition with aerodynamic and aeroelastic applications. In: XVII Congresso Nazionale AIDAA (Associazione Italiana Di Aeronautica e Astronautica), Roma, Italy.

Newmark, N.M., 1959. A method of computation for structural dynamics. ASCE Journal of Engineering Mechanics Division 85, 67–94.

Noack, B.R., Eckelmann, H., 1994. A low-dimensional Galerkin method for the three-dimensional flow around a circular cylinder. Physics of Fluids 6, 124–143.

Panikker, P.K.G., Lavan, Z., 1975. Flow past impulsively started bodies using Green functions. Journal of Computational Physics 18, 46–65.

Quartapelle, L., 1993. Numerical Solution of the Incompressible Navier–Stokes Equations. Birkhäuser, Basel.

Serrin, F., 1959. Mathematical principles of classical fluid mechanics. In: Flügge, S. (Ed.), Encyclopedia of Physics, Fluid Dynamics I, vol. VII/1. Springer, Berlin.

Son, J.S., Hanratty, T.J., 1969. Numerical solution for the flow around a cylinder at Reynolds number 40, 200 and 500. Journal of Fluid Mechanics 35, 369–386.

Thom, A., 1933. Flow past circular cylinders at low speeds. Proceedings of the Royal Society A 141, 651–669.

Wu, J.C., 1976. Numerical boundary conditions for viscous flow problems. AIAA Journal 14, 1042–1049.